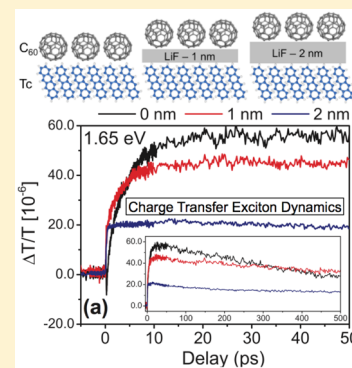


Tunable Charge Transfer Dynamics at Tetracene/LiF/C₆₀ InterfacesSiddharth Sampat,[†] Aditya D. Mohite,[‡] Brian Crone,[‡] Sergei Tretiak,[‡] Anton V. Malko,[†] Antoinette J. Taylor,[‡] and Dmitry A. Yarotski*[‡][†]Department of Physics, The University of Texas at Dallas, Richardson, Texas 75080, United States[‡]Los Alamos National Laboratory, Los Alamos, New Mexico 87545, United States

ABSTRACT: Ultrafast optical spectroscopy was utilized to investigate charge transfer dynamics across organic semiconductor tetracene/C₆₀ interfaces in the presence of a LiF barrier layer. Photoinduced absorption spectra in the 1.6–2.3 eV range reveal a strong effect of the intermediate LiF barrier layer on dynamics of the charge transfer excitons (CTE) creation and recombination. Increasing thickness of the LiF film from 0 to 1 nm significantly suppresses CTE recombination while CTE generation remains practically unaltered. Further increase of LiF thickness to 2 nm prevents creation of CTE by diffusion from tetracene but does not affect direct CTE excitation by incident photons. Unlike thin films studied here, direct CTE photogeneration at the interface between thick organic films accounts for a small fraction (as compared to diffusion-induced) of total CTE population, resulting in a larger contribution of the LiF barrier to charge separation efficiency.



INTRODUCTION

The prospects of low cost and large volume production of flexible electronic and optoelectronic devices such as solar cells and displays have fueled tremendous interest in organic semiconducting materials over the past few decades.^{1–4} Nevertheless, their practical applications are still limited due to relatively low electro-optical conversion efficiency of organic devices when compared with their inorganic counterparts.^{3,4} The key to high efficiency is minimization of parasitic losses of photoinduced charge carriers before they can be collected by the attached electrodes. Operation of organic solar cells relies on generation and subsequent dissociation of electrically neutral electron–hole bound states, excitons. Because exciton binding energies are rather high (~0.5 eV), thermally induced dissociation rates are lower than charge recombination rates, and a large portion of photoinduced charges is lost before reaching the electrodes. Charge separation can be significantly enhanced at the interfaces between two materials with cascaded energy structures, similar to inorganic semiconducting p–n junctions.^{3–5} Such heterostructures consist of “donor” (D) and “acceptor” (A) layers, which preferentially transport holes or electrons, respectively. Excitons are generated in the bulk of either D or A and then diffuse toward the interfacial region where they dissociate and create free charge carriers that diffuse toward collection electrodes. Preceding complete separation, closely spaced electrons in A and holes in D form a bound state, charge transfer exciton (CTE), which can either dissociate and generate photocurrent or recombine (radiatively or nonradiatively) and waste the photon that created it.⁶

Extensive studies have shown that the CTE dissociation/recombination ratio is one of the major factors that determine light harvesting or light emitting efficiency in organic devices. Therefore, multiple remedies to exciton and CTE losses have

been developed to improve charge separation and collection efficiencies using bulk heterojunctions,⁷ tandem stacking,⁸ and buffer layers with cascaded energy structure.^{5,9} Recently, Campbell and Crone demonstrated an almost 2-fold increase of photocurrent in organic photodiodes where tetracene (Tc, D) and C₆₀ (A) films were separated by a thin (1–2 nm) LiF layer (Figure 1b).¹⁰ This layer creates a tunneling barrier that reduces

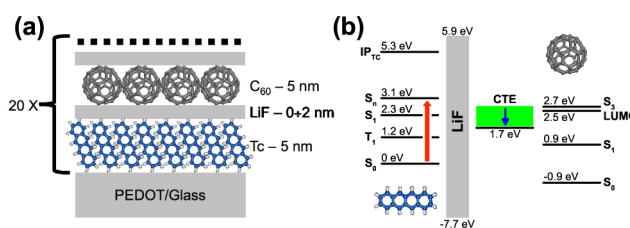


Figure 1. (a) Schematic representation of the sample heterostructure where 5 nm Tc and C₆₀ layers are separated by 0, 1, and 2 nm thick LiF barrier layer. (b) Schematic energy diagram of the Tc/LiF/C₆₀ interfaces^{10,21} showing that the electrons and holes from the photoexcited excitons in Tc and C₆₀, respectively, have to penetrate the tunneling barrier in order to produce the CTE and ensuing charge-separated states.

electron and hole wave function overlap in the CTE state and suppresses CTE recombination while simultaneously enhancing CTE dissociation due to lower CTE binding energy.^{10–12} At the same time, the barrier impedes initial exciton dissociation and effectuates an optimal LiF film thickness where these competing processes are balanced. Although a phenomenological model was

Received: September 22, 2014

Revised: December 18, 2014

Published: December 22, 2014

developed to provide quantitative description of the charge separation in such structures,^{11,12} the key parameters related to the dynamics of CTE formation and decay were only extracted indirectly, and no details were provided on the microscopic processes involved in the charge separation dynamics. However, observation and understanding the mechanisms underpinning femto- to picosecond CTE dynamics is essential for developing optimized D/barrier/A interfaces to enhance the performance of the next generation organic photovoltaic devices.

Ultrafast optical spectroscopy has emerged as a powerful tool for probing charge generation and separation^{13,14} in bulk and heterostructured organic semiconductors as well as competing processes in exciton/CTE evolution.^{15,16} This technique enables temporal discrimination of various relaxation pathways and coupling dynamics following gentle perturbation away from equilibrium by sub-100 fs optical pulses. In this article, we report on the dramatic effects that LiF tunneling barriers of various thicknesses have on the CTE dynamics at Tc/C₆₀ interfaces. These heterostructures can be described by existing phenomenological models^{11,12} and have also shown a potential for solar cell applications.¹⁷ Moreover, in both Tc and C₆₀ the basic exciton generation and recombination processes are relatively well understood,^{18–20,22} allowing us to concentrate only on CTE-related processes. Our results indicate that a large share of CTEs are generated almost instantaneously (within the 60 fs pulse width) while the rest are created through exciton diffusion to the interface within 2.5 ps. Importantly, introduction of a LiF tunneling barrier mostly affect the diffusion-induced CTE population, leaving the coherent/instantaneous part intact. The LiF layer also causes significant decrease in CTE recombination rates that explains enhanced photocurrent generation observed in time-averaged measurements.¹⁰

MATERIALS AND METHODS

The Tc/LiF/C₆₀ films for these studies were grown by thermal evaporation in an argon glovebox mounted vacuum evaporation system with separate sources for each material. Evaporations of all materials were done at or below 1 Å/s, at pressures below 10^{−7} Torr, without breaking vacuum between layers.¹⁰ To enhance optical response from the interfacial area, multilayered structures were created by stacking 20 periods of 5 nm Tc, 0–2 nm LiF, and 5 nm C₆₀ units on top of each other as shown in Figure 1a. To verify large-scale uniformity of the deposited films (especially, LiF layers), we performed ellipsometric measurements at multiple locations on thus-prepared samples, and all of them showed consistent layer thicknesses. All measurements were performed on these multilayered structured unless noted otherwise.

Ultrafast optical measurements were performed in a standard pump–probe transmission geometry and employed 50 fs pulses generated at 1.5 eV by a regenerative Ti:sapphire amplifier. Part of the amplifier output was sent to a nonlinear crystal to produce 70 fs pump pulses at 3.0 eV (well above the Tc absorption edge of 2.3 eV) which were then focused on the sample with a fluence of ~0.2–0.5 mJ/cm². The photoinduced absorption (PIA) was measured as transmission changes $-\Delta T/T$ of the probe pulses generated in an optical parametric amplifier. The pump beam intensity was modulated by the optical chopper, and a lock-in amplifier was used to detect the PIA with better than 5×10^{-6} sensitivity.

RESULTS AND DISCUSSION

Spectral and temporal variations of the $\Delta T/T$ signal from multilayer Tc/LiF/C₆₀ heterostructures (Figure 1) after photoexcitation are shown in Figure 2 for different thicknesses

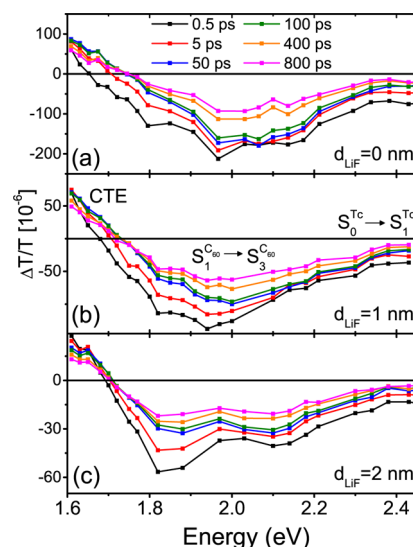


Figure 2. Transient transmission spectra acquired at several delays following photoexcitation of the Tc/LiF/C₆₀ heterostructures that consist of 20 Tc/C₆₀ repetition units separated by LiF barrier layer of different thickness $d_{\text{LiF}} = 0, 1, \text{ and } 2$ nm. CTE labels the location of the photoinduced charge transfer states, and $S_1^{\text{C}_{60}} \rightarrow S_3^{\text{C}_{60}}$ and $S_0^{\text{Tc}} \rightarrow S_1^{\text{Tc}}$ refer to electronic transitions between C₆₀ and Tc singlet exciton states, respectively, as shown in the energy diagram in Figure 1b.

($d_{\text{LiF}} = 0, 1, \text{ and } 2$ nm) of the LiF buffer film. The striking feature of these results is that they do not resemble well-known photoinduced absorption dynamics in either Tc^{18,19} or C₆₀^{20,22} films or crystals. For example, in thermally evaporated Tc films one would expect to observe fast (~10–50 ps) photobleaching dynamics around 2.3 eV arising from the depletion of the S_0^{Tc} exciton ground state.^{18,19} This bleaching should also be accompanied by a broad PIA peak around 1.9 eV due to $S_1^{\text{Tc}} \rightarrow S_N^{\text{Tc}}$ transitions.¹⁹ Although a similarly broad PIA peak at 2.0 eV is present in Figure 2, its decay time is significantly longer (~1.2 ns) than would be expected for S_1^{Tc} state depopulation by singlet–triplet fission and trapping (~10 ps). Moreover, PIA at 1.9 eV should have a lower amplitude than the bleaching at 2.3 eV due to the higher absorption cross section of S_0^{Tc} , which is clearly not the case in Figure 2. On the other hand, the broad PIA peak with a maximum at 1.8 eV and relaxation time of ~1.3 ns is a well-pronounced signature of the $S_1^{\text{C}_{60}} \rightarrow S_3^{\text{C}_{60}}$ transition in a C₆₀ singlet manifold.^{20,22} However, the photobleaching occurring at energies below 1.7 eV (Figure 2) is not intrinsic to C₆₀ film alone.

The observed $\Delta T/T$ dynamics in 1.6–2.4 eV range is therefore a result of a complex interplay between the relaxation processes occurring in the bulk of both Tc and C₆₀ films and near the interfaces between them. Careful comparison of the experimental results in Figures 2–4 with estimated CTE energies and films absorption allows us to attribute spectral features of $\Delta T/T$ signals from Tc/LiF/C₆₀ multilayers as follows. Figure 3 shows the transient transmission of a bilayer structure with a 10 and 50 nm Tc films topped with a C₆₀ layer of equal thickness. The photobleaching peak at 2.34 eV is clearly visible for 10 nm structure

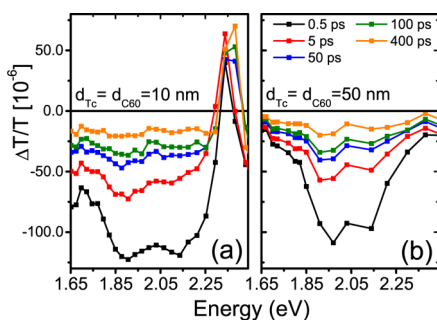


Figure 3. Spectrally resolved temporal evolution of the $\Delta T/T$ signal in the structure consisting of single 10 nm (a) and 50 nm (b) C_{60} film deposited on Tc layer of equal thicknesses.

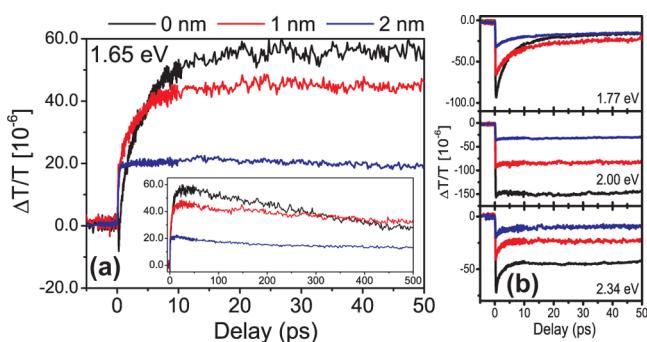


Figure 4. Time-resolved $\Delta T/T$ at selected probe energies taken in Tc/LiF/ C_{60} heterostructures with 0 nm (black), 1 nm (red), and 2 nm (blue) thickness of LiF barrier layer. Inset in (a) shows the dynamics in a wider delay range. The differences in $\Delta T/T$ decay dynamics for varying LiF thicknesses increases as CTE resonance near 1.7 eV is approached.

(Figure 3a) with energy and time scales that agree well with saturation of the $S_0^{Tc} \rightarrow S_1^{Tc}$ transition previously observed in Tc films.¹⁹ Unlike pure Tc films where relatively weak $S_1^{Tc} \rightarrow S_N^{Tc}$ PIA is observed below 2.2 eV, heterostructures exhibit broad PIA between 1.7 and 2.3 eV, with magnitude comparable to that of the bleaching signal at 2.3 eV. When the thicknesses of Tc and C_{60} are increased to 50 nm (Figure 3b), the bleaching peak disappears while the broadband PIA increases in magnitude. Therefore, these results demonstrate that the dynamics observed in multilayered structure is dominated by the C_{60} response that hinders Tc bleaching dynamics in the 1.9–2.4 eV range. Indeed, the absorption depth of C_{60} is more than 3 times smaller than that of Tc at a 3.0 eV pump photon energy ($d_{abs}^{Tc}(3 \text{ eV}) = 434 \text{ nm}$ vs $d_{abs}^{C_{60}}(3 \text{ eV}) = 144 \text{ nm}$),²⁴ leading to a significantly higher exciton population in C_{60} whose response obscures the photoinduced signal from Tc. Moreover, the decay time of 1.2 ns of the PIA in the 1.9–2.2 eV range agrees well with previously observed relaxation of $S_1^{C_{60}} \rightarrow S_3^{C_{60}}$ transient absorption changes. At probe energies around 2.3 eV, short-lived bleaching from Tc resonances competes with long-lived PIA from C_{60} and pushes $\Delta T/T$ to positive values as the thickness of C_{60} layer decreases. This is aided by an onset of long-lived photobleaching in C_{60} at energies above 2.45 eV.²² It is important to mention that charge-separated states of C_{60} do not influence these results because their absorption band lies at $\sim 1 \text{ eV}$.²³

Similarly, the photobleaching below 1.8 eV in multilayered structures emerges from the competition between the $S_1^{C_{60}} \rightarrow S_3^{C_{60}}$ PIA and stimulated emission from the photoinduced CTE population at the Tc/ C_{60} interfaces. The CTE binding energy may be estimated²⁵ from the ionization potential of Tc, IP_{Tc} ,

electron affinity of C_{60} , $EA_{C_{60}}$, and Coulomb stabilization energy of CTE state, $E_{C_{60}^-}^{Tc^+}$, using the relationship $E_{CTE} = IP_{Tc} + EA_{C_{60}} + E_{C_{60}^-}^{Tc^+}$. Knowing the values²⁴ of $IP_{Tc} = 5.3 \text{ eV}$ and $EA_{C_{60}} = -4.5 \text{ eV}$, and taking the stabilization energy¹² as $E_{C_{60}^-}^{Tc^+} = 0.1 \text{ eV}$, we can estimate $E_{CTE} \sim 0.9 \text{ eV}$ below LUMO of C_{60} . Stimulation from the probe pulse drives the recombination of the CTE state back to the neutral S_0^{Tc} and should produce stimulated emission at 1.7 eV and below (Figure 1). This value agrees very well with an onset of the PIA bleaching around 1.8–1.9 eV in Figure 2. In addition, comparison of the $\Delta T/T$ variation with LiF thickness d_{LiF} shows that despite close resemblance of the spectral responses in Figure 2, the time-resolved dynamics are dramatically affected by the LiF presence only around 1.7 eV (Figure 4). This is a clear indication of the interfacial origin of the signal in this spectral range. Indeed, the only change in $\Delta T/T$ at 2.0 and 2.34 eV is systematic decrease in the signal amplitude as d_{LiF} increases from 0 to 2 nm, while the rates and relative amplitudes of different components remain unaltered (Figure 4b). This behavior of “bulk” signals agrees well with simple reduction of the materials in the excitation volume and multiple reflections added by LiF interfaces. On the contrary, $\Delta T/T$ at 1.77 eV and especially 1.65 eV in Figure 4a exhibit not only the total amplitude change but also a great variation in dynamics rates and relative contributions from the various processes with increasing d_{LiF} . These arguments reliably identify the signal below 1.8 eV as coming primarily from the CTE state. Interestingly, thick (comparable to Tc film thickness) C_{60} layers employed in our experiments seem to enable direct observation of CTE response (sequentially amplified by multiple interfaces in the excitation volume) that is usually obscured by free charge PIA in structures where the ratio of D (Tc/Pc) to A (C_{60}) film thicknesses exceed 10 or more.¹⁴

Representative CTE dynamics at 1.65 eV is shown in Figure 4a as a function of LiF thickness. Three characteristic components can be clearly distinguished in all optical responses of the CTE state: initial fast ($\tau_{rf} < 100 \text{ fs}$) and slow ($\tau_{rs} = 2.5 \text{ ps}$) rises of $\Delta T/T$ magnitude are followed by the slow ($\tau_d > 1 \text{ ns}$) decay to equilibrium. The long relaxation times are consistent with the expected CTE lifetimes of few nanoseconds.^{10,12,24} The value of τ_d markedly increases when 1 nm LiF layer is added between Tc and C_{60} films, in agreement with previously observed and calculated exponential fall of the CTE recombination rate with increasing LiF thickness.^{10,12} The overall decay rate of CTE population consists of both dissociation and recombination processes, and it appears that recombination slowdown dominates changes in CTE dynamics, while the dissociation rate increases only slowly with LiF thickness and does not affect the total decay rate as much. Because of the relatively small delay range explored here, the increase in τ_d could not be quantified. No further increase of τ_d is observed when $d_{LiF} = 2 \text{ nm}$, which might be explained by the small variations of 10's ns signals over 500 ps delay range. However, the $\Delta T/T$ amplitude decreases monotonically as the LiF layer thickness is increased. This also correlates well with expected decrease in CTE population due to impeded exciton dissociation, i.e., charge separation, through the tunneling barrier between D and A.^{10,12}

The drop in CTE population should also be reflected in lower amplitude of the rise time dynamics which are associated with the formation of the CTE states. Surprisingly, increase of d_{LiF} affects only the amplitude of the 2.5 ps rise while 100 fs dynamics remains almost intact. CTE can be formed by (i) excitons diffusion from the bulk and dissociation at the interface,

(ii) electron transfer from the excitons in the interfacial region of donor material to manifold of CTE states that rapidly relax to the lowest energy CTE state, and (iii) direct excitation by incoming pump photons.^{6,15,16} The latter two processes (which we call direct vs diffusion-mediated CTE generation) occur on sub-picosecond time scales which are manifested as τ_{if} dynamics and are beyond the resolution of our experimental setup. The τ_{rs} component in CTE formation dynamic arises from the diffusion of singlet excitons in Tc because the diffusion length $L_d = (3D_S\tau_{rs})^{1/2} = 2.7$ nm (average $D_S = 1.1 \times 10^{-2}$ cm²/s)^{12,24,26} corresponds to half the Tc film thickness—the distance that exciton has to travel before dissociating at the interface. Exciton diffusion in C₆₀ is orders of magnitude slower and can be neglected. CTE generation from triplet excitons in Tc can also be neglected at these time scales because only small number of triplets are generated within 2.5 ps in the $S_1^{Tc} \rightarrow 2T_1^{Tc}$ fission process with an effective rate of 10 ps⁻¹.^{16,19} Moreover, in Tc $D_T \ll D_S$, but no slow rise (10's ps) dynamics is observed in Figure 4a that can be attributed to the triplet exciton diffusion process. Fast (<100 fs) dynamics in CTE formation must correspond to direct CTE excitation because only small fraction of Tc excitons are generated near the interface or can diffuse there within 100 fs, which contradicts an almost 50% contribution of the instantaneous process to the total CTE amplitude (compare red and blue curves in Figure 4a). Therefore, the LiF layer significantly decreases the number of CTE generated by the dissociation of singlet excitons that diffuse to the interface from the bulk of Tc. This agrees with an intuitive picture of the impeded exciton dissociation through the tunneling barrier as discussed before. Direct excitation should also be adversely affected by the tunneling barrier because the efficiency of this process depends on the wave function overlap between the hole in Tc and electron in C₆₀. However, no or very minor variations of the fast rise amplitude are observed in our measurements (Figure 4a) up to $d_{LiF} = 2$ nm and will require further attention in our future work.

CONCLUSIONS

We have directly observed interfacial charge transfer dynamics in Tc/LiF/C₆₀ multilayered heterostructures, where charge separation processes compete with parasitic radiative and nonradiative CTE recombination. Using ultrafast optical spectroscopy, we have demonstrated an appearance of the CTE bleaching at around 1.8 eV in the PIA spectra of these heterostructures. PIA clearly shows saturation of CTE population within 2.5 ps from photoexcitation and subsequent nanosecond recombination/relaxation into the charge-separated state. Unlike previously studied thick pentacene films interfaced with very thin C₆₀ layers where only charge-separated states of Pc were observed,¹⁴ our results indicate that dynamics of thick C₆₀ layers is more sensitive to CTE signatures in transient transmission spectra. This allowed us to demonstrate that addition of 1 nm LiF layer between Tc and C₆₀ layers significantly slows down CTE recombination and improves charge separation efficiency. On the other hand, thicker 2 nm LiF layers significantly reduce CTE density and decrease charge separation efficiency. An existence of optimal 1 nm < d_{LiF} < 2 nm is in good agreement with previously observed enhancement of the photocurrent in Tc/LiF/C₆₀ photovoltaic devices.¹⁰ Importantly, we have demonstrated that the rates of direct and diffusion-induced CTE formation can be separately controlled by an insertion of the barrier layer separating D and A sides in the device. These findings might have implications for development of more efficient organic photovoltaic and light-emitting devices.

AUTHOR INFORMATION

Corresponding Author

*E-mail: dzmitry@lanl.gov (D.A.Y.).

Notes

The authors declare no competing financial interest.

ACKNOWLEDGMENTS

This work was performed in part at the Center for Integrated Nanotechnologies, a U.S. Department of Energy, Office of Basic Energy Sciences (DOE BES) user facility, and funded by the Los Alamos National Laboratory Directed Research and Development program.

REFERENCES

- Heeger, A. J. *Semiconducting Polymers: The Third Generation*. *Chem. Soc. Rev.* **2010**, *39*, 2354–2371.
- Henson, Z. B.; Mullen, K.; Bazan, G. C. Design Strategies for Organic Semiconductors Beyond the Molecular Formula. *Nat. Chem.* **2012**, *4*, 699–704.
- Kumar, P.; Chand, S. Recent Progress and Future Aspects of Organic Solar Cells. *Prog. Photovoltaics* **2012**, *20*, 377–415.
- Schlenker, C.; Thompson, M. In *Unimolecular and Supramolecular Electronics I*; Metzger, R. M., Ed.; Topics in Current Chemistry; Springer: Berlin, 2012; Vol. 312, pp 175–212.
- Tan, Z.-K.; Johnson, K.; Vaynzof, Y.; Bakulin, A. A.; Chua, L.-L.; Ho, P. K. H.; Friend, R. H. Suppressing Recombination in Polymer Photovoltaic Devices via Energy-Level Cascades. *Adv. Mater.* **2013**, *25*, 4131–4138.
- Deibel, C.; Strobel, T.; Dyakonov, V. Role of the Charge Transfer State in Organic Donor-Acceptor Solar Cells. *Adv. Mater.* **2010**, *22*, 4097–4111.
- Dennler, G.; Sharber, M. C.; Brabec, C. J. Polymer-Fullerene Bulk-Heterojunction Solar Cells. *Adv. Mater.* **2009**, *21*, 1323–1338.
- Dou, L.; You, J.; Yang, J.; Chen, C.-C.; He, Y.; Murase, S.; Moriarty, T.; Emery, K.; Li, G.; Yang, Y. Tandem Polymer Solar Cells Featuring a Spectrally Matched Low-Bandgap Polymer. *Nat. Photonics* **2012**, *6*, 180–185.
- Kinoshita, Y.; Hasobe, T.; Murata, H. Control of Open-Circuit Voltage in Organic Photovoltaic Cells by Inserting an Ultrathin Metal-Phthalocyanine Layer. *Appl. Phys. Lett.* **2007**, *91*, 083518.
- Campbell, I. H.; Crone, B. K. Improving an Organic Photodiode by Incorporating a Tunnel Barrier Between the Donor and Acceptor Layers. *Appl. Phys. Lett.* **2012**, *101*, 023301.
- Liu, F.; Ruden, P. P.; Campbell, I. H.; Smith, D. L. Device Model for Electronic Processes at Organic/Organic Interfaces. *J. Appl. Phys.* **2012**, *111*, 094507.
- Liu, F.; Crone, B. K.; Ruden, P. P.; Smith, D. L. Control of Interface Microscopic Processes in Organic Bilayer Structures and Their Effect on Photovoltaic Device Performance. *J. Appl. Phys.* **2013**, *113*, 044516.
- Cabanillas-Gonzalez, J.; Grancini, G.; Lanzani, G. Pump-Probe Spectroscopy in Organic Semiconductors: Monitoring Fundamental Processes of Relevance in Optoelectronics. *Adv. Mater.* **2011**, *23*, 5468–5485 (2011).
- Rao, A.; Wilson, M. W. B.; Hodgkiss, J. M.; Albert-Seifried, S.; Bssler, H.; Friend, R. H. Exciton Fission and Charge Generation via Triplet Excitons in Pentacene/C₆₀ Bilayers. *J. Am. Chem. Soc.* **2010**, *132*, 12698–12703.
- Jailaubekov, A. E.; Willard, A. P.; Tritsch, J. R.; Chan, W.-L.; Sai, N.; Gearba, R.; Kaake, L. G.; Williams, K. J.; Leung, K.; Rossky, P. J.; Zhu, X.-Y. Hot Charge-Transfer Excitons Set the Time Limit for Charge Separation at Donor/Acceptor Interfaces in Organic Photovoltaics. *Nat. Mater.* **2013**, *12*, 66–73.
- Chan, W.-L.; Tritsch, J. R.; Zhu, X.-Y. Harvesting Singlet Fission for Solar Energy Conversion: One- Versus Two-Electron Transfer From the Quantum Mechanical Superposition. *J. Am. Chem. Soc.* **2012**, *134*, 18295–18302.

(17) Chu, C.-W.; Shao, Y.; Shrotriya, V.; Yang, Y. Efficient Photovoltaic Energy Conversion in Tetracene- C_{60} Based Heterojunctions. *Appl. Phys. Lett.* **2005**, *86*, 243506 (2005)..

(18) Thorsmølle, V. K.; Averitt, R. D.; Demsar, J.; Smith, D. L.; Tretiak, S.; Martin, R. L.; Chi, X.; Crone, B. K.; Ramirez, A. P.; Taylor, A. J. Morphology Effectively Controls Singlet-Triplet Exciton Relaxation and Charge Transport in Organic Semiconductors. *Phys. Rev. Lett.* **2009**, *102*, 017401.

(19) Burdett, J. J.; Müller, A. M.; Gosztola, D.; Bardeen, C. J. Excited State Dynamics in Solid and Monomeric Tetracene: The Roles of Superradiance and Exciton fission. *J. Chem. Phys.* **2010**, *133*, 144506.

(20) Dick, D.; Wei, X.; Jeglinski, S.; Benner, R. E.; Vardeny, Z. V.; Moses, D.; Srdanov, V. I.; Wudl, F. Transient Spectroscopy of Excitons and Polarons in C_{60} Films from Femtoseconds to Milliseconds. *Phys. Rev. Lett.* **1994**, *73*, 2760–2763.

(21) Zhu, X.-Y. How to Draw Energy Level Diagrams in Excitonic Solar Cells. *J. Phys. Chem. Lett.* **2014**, *5*, 2283–2288 textbf.

(22) Farztdinov, V. M.; Dobryakov, A. L.; Letokhov, V. S.; Lozovik, Yu. E.; Matveets, Yu. A.; Kovalenko, S. A.; Ernsting, N. P. Spectral Dependence of Femtosecond Relaxation and Coherent Phonon Excitation in C_{60} . *Phys. Rev. B* **1997**, *56*, 4176–4185.

(23) Guldi, D. M.; Prato, M. Excited-State Properties of C_{60} Fullerene Derivatives. *Acc. Chem. Res.* **2000**, *33*, 695–703.

(24) Pope, M.; Swenberg, C. E. *Electronic Processes in Organic Crystals and Polymers*; Oxford University Press: New York, 1999.

(25) Yi, Y.; Coropceanu, V.; Bredas, J.-L. Exciton-Dissociation and Charge-Recombination Processes in Pentacene/ C_{60} Solar Cells: Theoretical Insight into the Impact of Interface Geometry. *J. Am. Chem. Soc.* **2009**, *131*, 15777–15783 (2009)..

(26) Vaubel, G.; Baessler, H. Diffusion of Singlet Excitons in Tetracene Crystals. *Mol. Cryst. Liq. Cryst.* **1970**, *12*, 47–56.